Hindawi
Advances in Civil Engineering
Volume 2018, Article ID 3245624, 16 pages
https://doi.org/10.1155/2018/3245624

*Research Article*

# Additional Stress on a Buried Pipeline under the Influence of Coal Mining Subsidence

**Ping Xu, Minxia Zhang, Zhibin Lin, Zhengzheng Cao, and Xu Chang**

*School of Civil Engineering, Henan Polytechnic University, No. 2001 Shiji Road, Shanyang District, Jiaozuo, Henan 454000, China*

Correspondence should be addressed to Minxia Zhang; zhangminxia@126.com

Received 30 December 2017; Revised 24 March 2018; Accepted 26 April 2018; Published 11 June 2018

Academic Editor: Chiara Bedon



Buried pipelines influenced by coal mining subsidence will deform and generate additional stress during surface deformation. On the basis of the coordinating deformation relationship between buried pipeline and its surrounding soils, a stress analysis method of a buried pipeline induced by mining was proposed. The buried pipeline additional stresses were analyzed; meanwhile, a corresponding analysis process of the pipeline stresses was also presented during mining subsidence. Furthermore, based on the ground subsidence along the pipeline predicted in advance by the probability integral method, the additional stresses and Von Mises equivalent stresses and their distributions along the buried pipeline induced by the exploitation of a coal mining working face named 14101 were obtained. Meanwhile, a comparative analysis of additional stresses between simulation and analytical calculation was performed for the deep analysis and reliability of the results presented by the proposed methodology in this paper. The proposed method provides references for analysis of the additional stress and safety of buried pipelines under the influence of mining subsidence.

## 1. Introduction

Extending large-scale surface subsidence induced by underground coal mining has appeared in coal mining areas. Therefore, buried pipelines are prone to deformations although seemingly keeping far away from the mining goafs [1, 2]. The most significant problems to buried pipelines near coal mining are the additional stress and safety induced by coal exploitation during mining subsidence. Unfortunately, the effective methodology of additional stress analysis of buried pipelines cannot be proposed because of the unobtainable constraining forces from the surrounding subsidence soil to the pipelines. Therefore, it is very important to present a practicable methodology to evaluate the additional stress and safety of buried pipelines under the influence of mining subsidence.

It is well known that the additional stresses and deformations of a buried pipeline are induced by the constraining force from surrounding soil mass during surface subsidence. Therefore, additional stress analysis of a buried pipeline affected by mining subsidence should take the relationship of pipe-soil coordinating deformation into account firstly. As a matter of fact, the surface deformations along a pipeline could be predicted in advance through the probability integral method, if subsidence prediction parameters of a mine are given [3–5]. This paper tries to start with the analysis of the relationship of pipe-soil coordinating deformation and then combines the surface deformation along the buried pipeline and subsidence prediction parameters to present an available additional stress analysis method of buried pipeline affected by mining subsidence.

## 2. State of the Art

The stress analysis and response of buried pipelines induced by surface deformations caused by the landslide, faulting, and excavation of foundation pits and tunnels have been studied extensively. Joshi et al. [6] proposed a simple finite element model to analyze buried pipeline subjected to reverse fault motion, which uses beam elements for the pipeline and discrete nonlinear springs for the soil. Zheng et al. [7] discussed the stress and deformation characteristics of a buried pipeline under the influence of the landslide.

Yu, Zhang, and Wu evaluated the stress and safety of buried pipelines during tunnel construction through laboratory test, numerical simulation analysis, field observation, and pipeline-soil interaction analysis [8–10]. Prendergast and Gavin [11] treated a buried pipeline as a short beam on an elastic foundation and analyzed its additional stress distribution. The above studies mainly analyzed the pipeline stresses by using the elastic foundation beam method which is too difficult to obtain actual constraints from pipeline surrounding soil especially in the disturbed soil mass.

Peng and Luo proposed a method to predict the subsidence damages to buried thin pipelines. It was found that the major contributors to the pipeline stress were the horizontal strain and vertical curvature [12]. Malinowska discussed the influences of continuous surface deformation on buried pipelines and analyzed the potential risks of buried pipelines during mining subsidence based on GIS (geographic information system) to understand the effect of mining subsidence on buried pipelines [13, 14]. Wang et al. deduced the compatibility equations of axial physical and geometric extending deformations of a buried pipeline by analyzing the stress characteristics of the pipeline in a subsidence zone [15]. Their researches provided important references for the stress analysis of pipelines in mining subsidence zone. However, the existing researches on additional stress analysis of buried pipelines have not considered the evolution and relationship of pipe-soil coordinating deformation.

In this paper, a methodology of additional stress analysis of a pipeline is presented according to the relationship of pipe-soil coordinating deformation. Furthermore, a corresponding analysis process is also proposed by combining the surface deformation along the buried pipeline which could be obtained in advance by the given prediction parameters of mining subsidence. The proposed method provides references for analysis of the additional stress and safety of buried pipelines under the influence of mining subsidence.

The remainder of this paper is organized as follows. Section 3 establishes the relationship of pipe-soil coordinating deformation and mechanical model and then proposes a corresponding analysis process of the pipeline stresses. Section 4 discusses the applicability of the method through a case study combining with the contrastive analysis from simulation. Section 5 summarizes the conclusions.

## 3. Methodology

*3.1. Relationship of Pipe-Soil Coordinating Deformation under Mining Subsidence.* Engineering practice shows that the continuous moving surface subsidence is located in circumjacent zones of the coal mine goafs [16], and this surface subsidence is more prone to affect the buried pipelines near the goafs because this deformation has a considerably large influence scope. Therefore, this paper mainly focuses on the additional stress analysis of a buried pipeline influenced by this continuous surface subsidence.

The surrounding soil mass is both a load and constraint medium to the pipeline. The test results of modeling experiments showed that deformation between the buried pipeline and its surrounding soil mass can be divided into pipeline-soil coordinating deformation (PSCD) and pipeline-soil noncoordinating deformation (PSNCD) according to the internal consistency of deformations between buried pipeline and its surrounding soil mass during mining subsidence [17, 18]. If subsidence is small or pipeline is far away from the subsidence areas, the deflection of the pipeline is equal to the sinking values of surface, it is in the PSCD stage as shown in Figure 1(a), and the bottom of the pipeline is always supported by the surrounding soil mass at this stage. However, given the high deformation rigidity of the buried pipeline, if surface subsidence is bigger or pipeline is near the subsidence areas, the sinking values of soil under the pipeline are always greater than the pipeline deflection, and PSNCD appeared at the center zone of the pipeline affected by mining subsidence as shown in Figure 1(b). Therefore, there is no support force from the soil beneath the pipeline at this zone.

The subsidence of the buried pipeline is basically consistent with its surrounding soil mass at the PSCD stage as shown in Figure 1(a). Therefore, soil subsidence along the pipeline is viewed as the deflection of the pipeline in mechanical analysis. However, the noncoordinating deformation will appear between the pipeline and its surrounding soil mass in the middle of the subsidence area at the PSNCD stage, while the coordinating deformation will be always maintained at the two edges of the subsidence area as shown in Figure 1(b). Therefore, regions along the pipeline should be divided into PSCD and PSNCD zones in the mechanical analysis.

The constraining force along the axial direction of the buried pipeline such as the pipeline-soil frictional force influences the pipeline-soil coordinating subsidence slightly and so can be neglected when analyzing the pipeline-soil coordinating bending deformation during surface subsidence. Therefore, stresses along the pipeline during PSCD analyzed are shown in Figure 2.

There is a pipeline coordinate system ($O_1x_1y_1$) as shown in Figure 2, and the intersection point between the edge of subsidence basin and the buried pipeline is used as the origin. The pipeline direction is the $x_1$-axis, and the vertical direction is the $z_1$-axis. The overlying soil gravity on the pipeline at any point, which is $l$ distant from the origin, is $q_s$; the pipeline gravity is $q_g$; and $f(l)$ is the support force of surrounding soil mass to the pipeline. During the pipeline-soil coordinating subsidence, a mechanical analysis of the pipeline could be calculated as a continuous beam [6, 8, 9]. According to bending theory of continuous beam, the following equation can be obtained:

$$EI\frac{d^4W}{dl^4} = q_s + q_g - f(l), \tag{1}$$

where $E$ is the elastic modulus of the buried pipeline, $I$ is the inertial moment of the buried pipeline, and $W$ is the deflection of the buried pipeline. The analysis of the buried pipeline deformation features under mining subsidence reveals that surface deformations at any point along the pipeline can be considered as the corresponding pipeline deflection $W$ during the PSCD process.

Given the constraining force of the surrounding soil mass, the pipeline is deformed with the surface during early surface deformation. However, given the antibending rigidity of

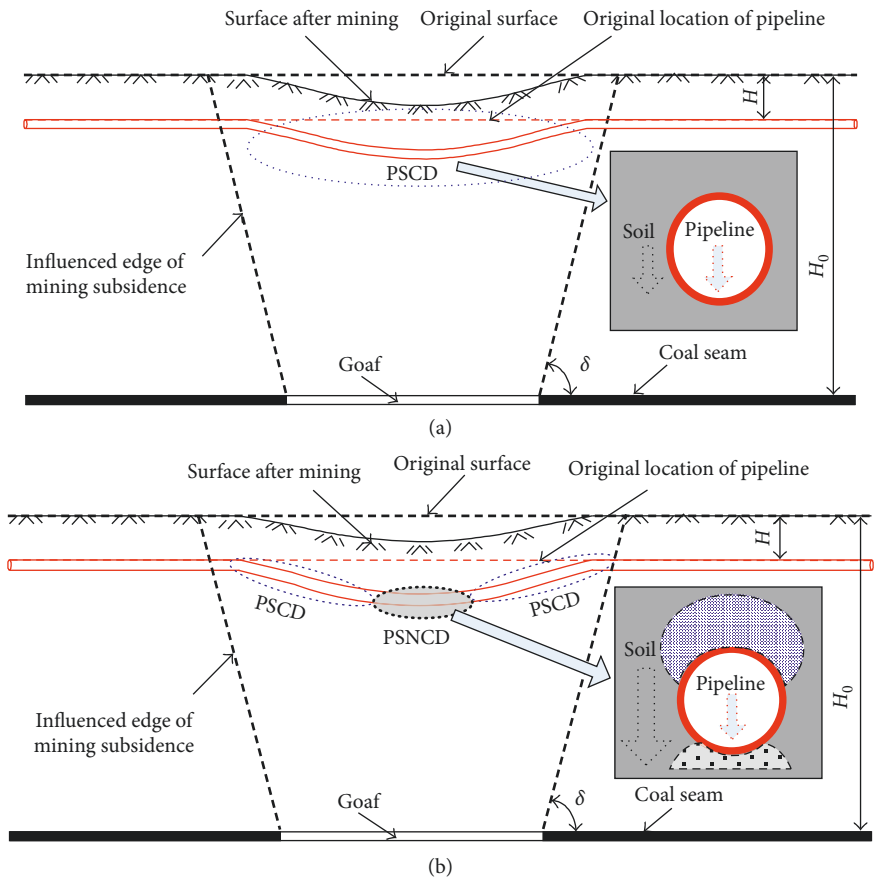


Figure 1: Deformation developments of a buried pipeline and its surrounding soil during mining subsidence: (a) PSCD stage during subsidence and (b) PSNCD stage during subsidence.

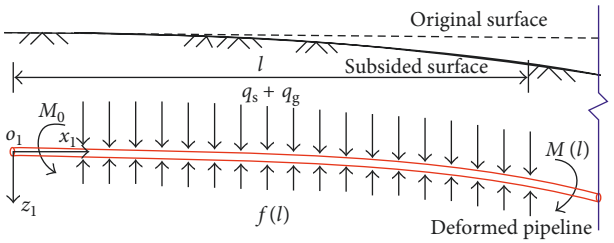


Figure 2: Stresses under pipeline-soil coordinating deformation.

buried pipeline is significantly higher than its surrounding soil mass, $f(l)$ will decrease gradually with increasing surface deformation. Subsequently, there is a critical state between PSCD and PSNCD while $f(l) = 0$. Therefore, the equation of the critical state for PSCD from (1) is as follows:

$$EI\frac{d^4W}{dl^4} = q_s + q_g, \tag{2}$$

where the calculation formulas of $q_s$ and $q_g$ are as follows:

$$\begin{aligned} q_s &= \rho_s g H D, \\ q_g &= \rho_g g \pi D S, \end{aligned} \tag{3}$$

where $\rho_s$ is the soil mass density, $g$ is the acceleration of gravity, $H$ is the buried depth of the pipeline, $\rho_g$ is the average density of the pipeline, $S$ is the wall thickness of the pipeline, $D$ is the outer diameter of the pipeline, and the remaining parameters are the same as above.

*3.2. Surface Deformation Analysis along the Pipeline.* Mechanical analysis models proposed in this paper are used to obtain additional stresses of pipeline based on the pipeline deformation which is other than the elastic foundation beam models [19, 20]. A geometric relationship of the deformations between subsidence surface and buried pipeline should be established firstly to analyze the deformation and additional stresses along the buried pipeline effectively.

To analyze the geometric relationship between surface deformation caused by mining subsidence and the buried pipeline deformation, three coordinate systems are established: surface, coal seam, and pipeline coordinate systems. The surface coordinate system is a global coordinate system, and the two others are local coordinate systems. The relationship among the coal seam ($O_2st$), surface ($Oxy$), and pipeline coordinate systems ($O_1x_1y_1$) is shown in Figure 3. When long-well caving exploitations are adopted during coal mining, the working faces are usually a rectangle with the dip length is $L_1$, the strike length is $L_2$, and the exploitation range is $O_2CDE$ in the plane in the coal seam coordinate system.

The included angle between the buried pipeline and $x$-axis of the surface coordinate system is $\theta$. In the pipeline

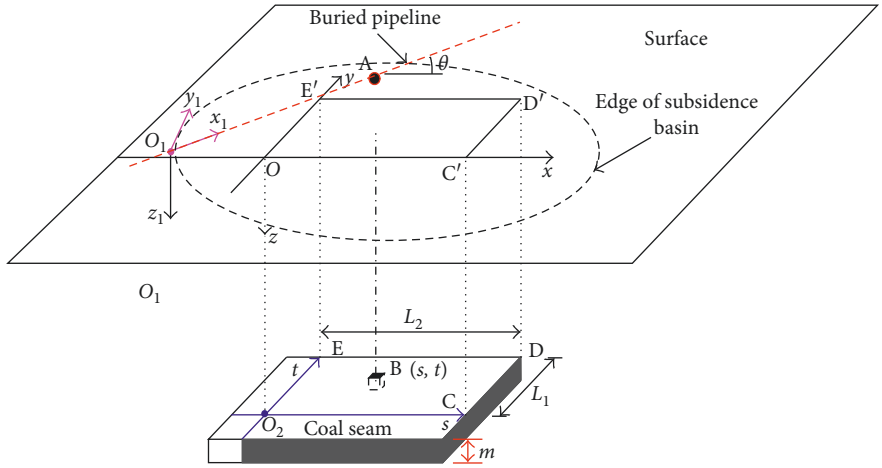


Figure 3: Surface, pipeline, and coal seam coordinate systems.

coordinate system, the point of the intersection between buried pipeline and edge line of the mining subsidence basin is the origin ($o_1$). The axial direction of the pipeline is utilized as the $x_1$-axis. If the $o_1$ coordinates in the surface coordinate system are $(X, Y)$, then the coordinates of any point in the subsidence zone, where is $l$ away from $o_1$, could be calculated according to the transformation formulas of coordinates:

$$\begin{aligned} x &= X + l \cdot \cos\theta, \\ y &= Y + l \cdot \sin\theta. \end{aligned} \tag{4}$$

During coal mining (Figure 3), subsidence of any point on the surface along the pipeline could be gained according to the probability integral method which is extensively recommended by correlative regulations of mining subsidence prediction as follows [3, 4, 16]:

$$W(l,\ \theta) = \frac{1}{W_0} W^0(X + l \cdot \cos\theta) W^0(Y + l \cdot \sin\theta), \tag{5}$$

where $W_0 = mq\cos\alpha$ is the maximum subsidence during coal mining, $m$ is the coal seam thickness, $q$ is the subsidence coefficient, and $\alpha$ is the dip angle of the coal mining.

The horizontal surface displacement along the pipeline can be divided into axial and horizontal components. The surface subsidence can be obtained in advance by prediction according to the probability integral method [3, 4, 16], and the horizontal surface displacement at any point along the pipeline is as follows:

$$\begin{aligned} U(l,\ \theta) = \frac{1}{W_0}\Big[ & U^0(X + l \cdot \cos\theta) W^0(Y + l \cdot \sin\theta)\cos\theta \\ & + U^0(Y + l \cdot \sin\theta) W^0(X + l \cdot \cos\theta)\sin\theta \Big], \end{aligned} \tag{6}$$

$$\begin{aligned} U\left(l,\ \theta + \frac{\pi}{2}\right) = \frac{1}{W_0}\Big[ & U^0(Y + l \cdot \sin\theta) W^0(X + l \cdot \cos\theta)\cos\theta \\ & - U^0(X + l \cdot \cos\theta) W^0(Y + l \cdot \sin\theta)\sin\theta \Big], \end{aligned} \tag{7}$$

where $W^0(x)$ and $U^0(x)$ are the calculation formulas of subsidence and horizontal displacement at any surface point in finite mining. The formulas $W^0(x)$ and $U^0(x)$ could be obtained from published literatures [16, 17].

The surface subsidence along the pipeline obtained by the probability integral method is substituted in (1). If $f(l)$ is always greater than zero, it shows a support force exists around the pipeline, that is to mean the subsidence deformation along the pipeline is all PSCD. Otherwise, there is a critical state between PSCD and PSNCD while $f(l) = 0$, and the critical points of PSCD and PSNCD will be determined by (2).

*3.3. Additional Bending Stress of a Buried Pipeline in the PSCD Stage.* Mining surface deformation can be divided into horizontal displacement $V(s)$ and vertical displacement $W(s)$. During the stress analysis of buried pipeline under mining influences, the buried pipeline can be deemed as a bending continuous beam. In the PSCD zone, soil mass deformation is the deflection of buried pipeline. Therefore, the additional bending moments $M_y(l)$ and $M_z(l)$ are as follows:

$$\begin{aligned} M_y(l) &= EI\frac{\partial^2 V(s)}{\partial s^2}, \\ M_z(l) &= EI\frac{\partial^2 W(s)}{\partial s^2}. \end{aligned} \tag{8}$$

The spatial bending deformation of the buried pipeline is the superposition of the $W(s)$ and $V(s)$. It worth to mention that $W(s)$ is the $W(l,\ \theta)$ as shown in (5) and $V(s)$ is the superposition of the $U(l,\ \theta)$ and $U(l,\ \theta + (\pi/2))$ as shown in (6) and (7) if it is in the PSCD stage.

According to superposition theory, if the $M_y(l)$ and $M_z(l)$ are deduced by (8), the spatial resultant bending moment and bending stress are as follows:

$$\begin{aligned} M(l) &= \sqrt{M_y^2(l) + M_z^2(l)}, \\ \sigma_n^M(l) &= \frac{M(l)\rho}{I}. \end{aligned} \tag{9}$$

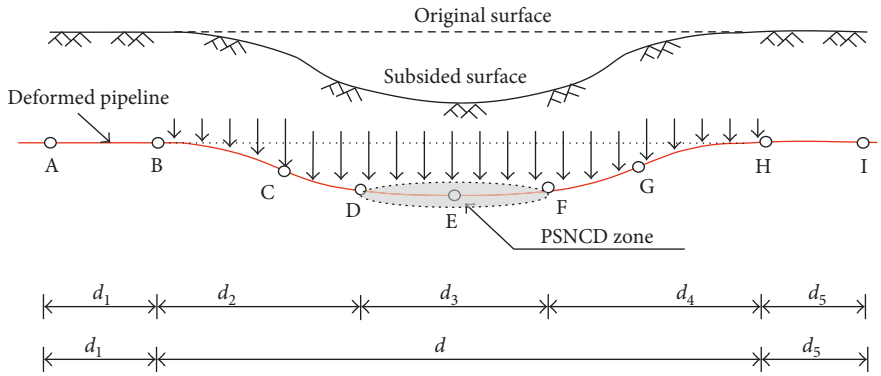


Figure 4: Buried pipeline in the PSNCD stage.

*3.4. Additional Bending Stress in the PSNCD Stage.* The bending pipeline deformation at the PSNCD stage is shown in Figure 4. Section BH is the zone of surface mining subsidence coverage with length $d$. Section AI is the influence zone of the buried pipeline. Sections AB and HI only show axial pipeline-soil frictional force and do not generate bending deformation. The bending deformation of the buried pipeline only occurs in section BH. Section BH can be further divided into PSNCD section (DF) and PSCD sections (BD and FH). The bending stress in section DF can be simplified as a continuous beam model. The mechanical analysis indicates that section DF can be viewed as a hidden-hanging buried pipeline that only exhibits equivalent uniform load $q$ on the top, but no support force from the bottom soil mass (Figure 5).

A coordinate system $Oxy$ for the PSNCD section was established (Figure 5) to analyze the internal stresses on the PSNCD section. The load $q$ is the equivalent uniform load on the top pipeline including the dead loads of the pipeline and transmission medium and the constraining force of soil mass to the pipeline during subsidence. The deflection, bending moment, corner, shearing force, and axial force at point D are $l_0$, $M_0$, $\theta_0$, $Q_0$, and $N_0$, respectively. $d_3$ is the length of hidden-hanging section. Subsequently, one microunit is obtained from section DF as shown in Figure 6.

According to the force analysis shown in Figure 6, equilibrium conditions of the microunit are as follows:

$$\begin{aligned} N + dN - N &= 0, \\ Q + dQ - Q + q \cdot dx &= 0, \\ M + dM - M - Q \cdot dx + N \cdot dy - \frac{1}{2} q (dx)^2 &= 0. \end{aligned} \tag{10}$$

Therefore,

$$\begin{aligned} dN &= 0, \\ \frac{dQ}{dx} &= -q, \\ \frac{dM}{dx} - Q + N \cdot \frac{dy}{dx} &= 0. \end{aligned} \tag{11}$$

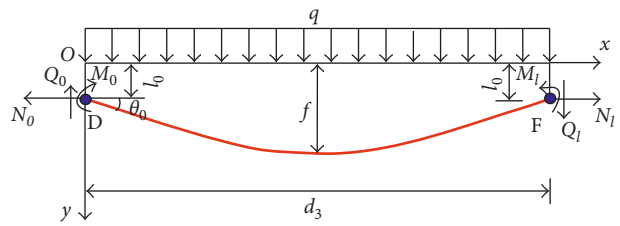


Figure 5: Stress on the PSNCD section.

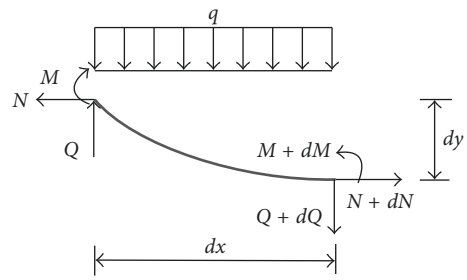


Figure 6: Force analysis of the microunit obtained from section DF.

Taking a derivative of the third equation in (11) with respect to $x$, then it is substituted in the second equation. Subsequently, the governing differential equation of section DF is as follows:

$$\frac{d^2 y}{dx^2} + \frac{1}{N} \frac{d^2 M}{dx^2} = -\frac{q}{N}, \tag{12}$$

where $M = -EI\,(d^2 y/dx^2)$. The differential equation of the bending deformation of section DF is as follows:

$$\frac{d^4 y}{dx^4} - \frac{N}{EI} \frac{d^2 y}{dx^2} - \frac{q}{EI} = 0. \tag{13}$$

Let $k = \sqrt{N/EI}$, so the solution to (13) can be obtained as follows:

$$y(x) = \frac{C_1 sh(kx)}{k^2} + \frac{C_2 ch(kx)}{k^2} - \frac{qx^2}{2EIk^2} + C_3 x + C_4. \tag{14}$$

On the basis of the boundary conditions of section DF, namely, $y(0) = l_0$, $y'(0) = \theta_0$, $y(d_3) = l_0$, and $y'(d_3) = -\theta_0$, the following equation is derived:

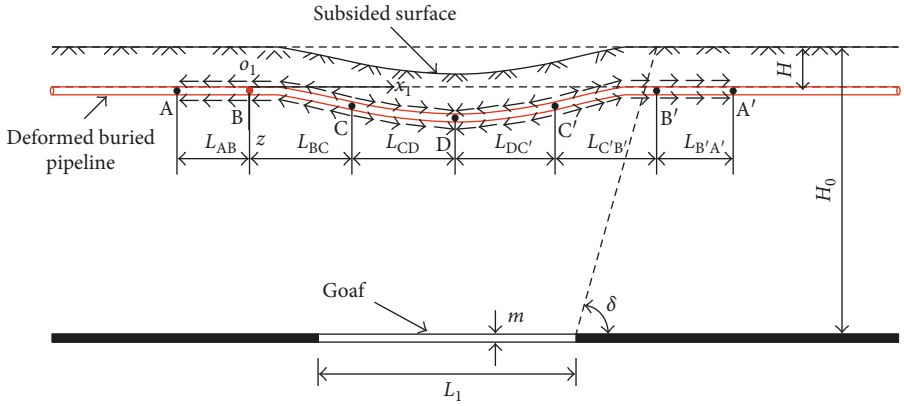


Figure 7: Distribution of frictional force along the pipeline in the subsidence zone.

$$C_1 = \frac{(qd_3 - 2EI\theta_0 k^2)(1 + ch(kd_3))}{2EIk^3 sh(kd_3)},$$

$$C_2 = \frac{\theta_0}{k} - \frac{qd_3}{2EIk^3},$$

$$C_3 = l_0 - \frac{(qd_3 - 2EI\theta_0 k^2)(1 + ch(kd_3))}{2EIk^3 sh(kd_3)}, \quad (15)$$

$$C_4 = \frac{qd_3}{2EIk^2}.$$

Equation (15) is substituted in (14) to obtain the deflection equation of section DF as follows:

$$y(x) = l_0 - \frac{qx^2}{2EIk^2} + \frac{d_3 qx}{2EIk^2} - \frac{(2EIk^2\theta_0 - d_3 q)[ch(kx)cth(kd_3/2) - sh(kx) - cth(kd_3/2)]}{2EIk^3}. \quad (16)$$

Therefore, the bending moment equation of section DF can be obtained as follows:

$$M = \frac{q}{k^2} + \frac{(-d_3 q + 2EIk^2\theta_0)[ch(kx)cth(kd_3/2) - sh(kx)]}{2k}. \quad (17)$$

On the basis of the first-order derivation of the bending moment $M$, the shearing force of section DF is as follows:

$$Q(x) = \frac{(d_3 q - 2EIk^2\theta_0)[ch(kx) - cth(kd_3/2)sh(kx)]}{2}. \quad (18)$$

In (10)–(18), $d_3$ is the length of section DF, which could be determined by the scope of mining influence and PSCD conditions. $M_0$, $N_0$, and $l_0$ at point D could be calculated according to the continuous conditions of the buried pipeline.

*3.5. Additional Axial Pipeline-Soil Frictional Force.* Because of the different physical and mechanical properties between the buried pipeline and its surrounding soil mass during subsidence, an additional frictional force in the pipeline-soil interface will be generated to prevent against pipeline-soil relative movements at the axial direction of the buried pipeline. It is assume that the length of the buried pipeline influenced by pipeline-soil frictional force is A-A′ during mining subsidence. What is more, the edge of the surface subsidence zone is above point B, and the bending deformation of one subsidence section is symmetric at point D (Figure 7). The left pipeline subsidence is analyzed in the following text. Although section AB of the buried pipeline is stretched by the subsidence zone, subsidence deformation exerts no influence to the surrounding soil mass; accordingly, the pipeline-soil frictional force pointing to the non-subsidence zone along the axial line of the buried pipeline is generated (Figure 7). The horizontal soil mass deformation in section BC increases from the edge to the inside part of the subsidence curve. Assuming that the moving deformation of the surrounding soil mass at point C is equal to the tensile deformation of the pipeline, then the pipeline-soil frictional force at point C is zero. The horizontal deformation of the surrounding soil mass in section CD pointing to the center of the subsidence zone is larger than the pipeline deformation; therefore, the pipeline-soil frictional force in section CD pointing to the subsidence curve center along the buried pipeline would be generated. When the stress-strain relationship (constitutive equation) of the buried pipeline is known, the positions of the above characteristic points (A, B, C, and D) could be determined by combining the calculated results of mining surface deformation along the buried pipeline as detailed above. On this basis, the distribution of the pipeline-soil frictional force would be acquired while the deformations of the surface along the pipeline are deduced by (2)–(4) and the stress-strain relation relationship of the material of pipe given in advance.

Nyman [21] assumes that frictional force will reach its limit value when the pipeline-soil relative displacement increases to the yield displacement $x_u$ (generally at 3–10 mm). Taking into consideration the sufficiently large surface subsidence compared to $x_u$, it is assumed that pipeline-soil relative displacement is larger than the yield displacement in general during the mining subsidence process. Therefore, the frictional force along the pipeline should be regarded as an ultimate frictional force for simplification. According to ASCE's formulas of the pipeline-soil ultimate frictional force

per unit length of the buried pipeline [21, 22], the frictional force is as follows:

$$f_u = \pi D k' c_s + 0.5\pi D H' \rho_s g (1 + K_0) \tan \psi, \quad (19)$$

$$k' = 0.608 - 0.123 c_s - \frac{0.274}{c_s^2 + 1} + \frac{0.695}{c_s^3 + 1}, \quad (20)$$

where $k'$ is the adhesion coefficient, $c_s$ is the cohesion coefficient of the surrounding soil mass, $H'$ is the distance between the surface and axial line of the pipeline, $\rho_s$ is the soil mass density, $g$ is the acceleration of gravity, $K_0$ is the coefficient of static earth pressure, $\psi$ is the pipeline-soil frictional angle ($\psi = f' \cdot \varphi$), $\varphi$ is the internal frictional angle of soil mass, $f'$ is the coefficient of the pipeline interface, and the remaining parameters are the same as above. Eventually, the axial frictional force will be determined based on the distribution of the pipeline-soil frictional force and its simplified empirical equation (19).

Finally, considering the effect of bending and pipeline-soil friction on the buried pipeline under mining subsidence, the additional stress of the pipeline $\sigma_n^*$ is obviously composed of axial bending stress and axial frictional force which is as follows:

$$\sigma_n^* = \sigma_n^M (l) + \sigma_n^f (l). \quad (21)$$

*3.6. Initial Stress of the Buried Pipeline.* The transmission media in the buried pipeline are mainly oil or gas under pressure. The main initial stresses on the pipelines during the service period mainly include initial soil pressure, internal pressure from transmission media, and thermal stress. Given that oil or gas pipelines are buried shallowly, the initial stress caused by the initial soil pressure is small and could be neglected. Oil or gas internal pressure is one of the main influencing factors of pipeline operation and stress state. Buried oil or gas pipelines are generally thin-wall pipes, in which hoop, axial, and radial stresses are generated by the internal pressure [23]:

$$\sigma_\theta = \frac{PD}{2S}, \quad (22)$$

$$\sigma_h = \mu \sigma_\theta = \mu \frac{PD}{2S}, \quad (23)$$

$$\sigma_r = \frac{d^2 - (d^2 D^2 / r^2)}{D^2 - d^2} \sigma_\theta, \quad (24)$$

where $\sigma_\theta$, $\sigma_h$, and $\sigma_r$ are, respectively, the hoop, axial, and radial stresses caused by internal pressure; $P$ is the internal pressure; $S$ is the wall thickness of the pipeline; $\mu$ is the Poisson ratio of the material of the pipeline; $d$ is the inner diameter of the pipeline; $r$ is the radial position of the calculation point; and the remaining parameters are the same as above. Thermal stress is caused by the temperature difference between the operation and construction environments of the pipeline. Reference states that the axial stress caused by temperature difference is as follows [23]:

$$\sigma_n^T = \xi E \Delta T, \quad (25)$$

where $\xi$ is the linear expansion coefficient of the pipeline, $E$ is the elastic modulus of the buried pipeline, and $\Delta T$ is the temperature changes in the pipeline.

Pipeline initial stresses can be divided into axial, hoop, and radical components. The initial axial stress $\sigma_L'$ is parallel to the axial line of the pipeline and mainly caused by internal pressure and thermal stress:

$$\sigma_L' = \sigma_h + \sigma_n^T. \quad (26)$$

With the previous analysis, the additional stress of the pipeline shown in (21) is composed of axial bending stress and axial frictional force, and the initial axial stress shown in (26) is composed of axial internal pressure stress and axial thermal stress. Therefore, the ultimate axial stress $\sigma_L$ on buried pipeline will be determined by combining (21) with (26) during mining subsidence which is as follows:

$$\sigma_L = \sigma_h + \sigma_n^T + \sigma_n^M (l) + \sigma_n^f (l). \quad (27)$$

Of course, Von Mises equivalent stress of any cross section which is more suitable for safety assessment to the deformed buried pipeline could be calculated according to the calculation formulas of hoop and radical and axial stresses caused by combined effects of the initial stress and additional stress induced by mining subsidence.

In conclusion, on the basis of the above analysis, a comprehensive mechanical response analysis procedure of the buried pipeline under mining subsidence influences could be presented which is shown in Figure 8.

As previously analyzed, the surface deformation along the buried pipeline and a judgment of the pipeline-soil deformation (coordinating or noncoordinating deformation) should be determined firstly based on the coal mining parameters, pipeline parameters, and surrounding soil parameters. Subsequently, on the basis of the coordinating deformation relationship between buried pipeline and its surrounding soils, the additional stress of the pipeline including bending stress and pipeline-soil frictional force could be deduced. Eventually, Von Mises equivalent stress and assessment of the pipeline mechanical response under mining subsidence could be proposed by combining the additional and initial stresses on the buried pipeline.

## 4. Engineering Case Study

*4.1. Brief Introduction to the Engineering Project.* The coal mine selected for this study is located in Shuozhou city, Shanxi Province. The first working face of this coal mine is called 14101, which displays a rectangular shape. Single-strike, long-wall comprehensive mechanization coal caving was adopted, and the roof on the goaf collapsed naturally. The basic conditions of the working face are listed in Table 1. A buried natural gas pipeline constructed near the subsidence area would be affected by the coal mining of the working face 14101. In this area, there are no block valve chambers or anchor blocks or fixed anchorages along the natural gas pipeline. The shortest horizontal distance between the open-off cut of the working face and pipeline was approximately 116 m, and the advancing direction of the

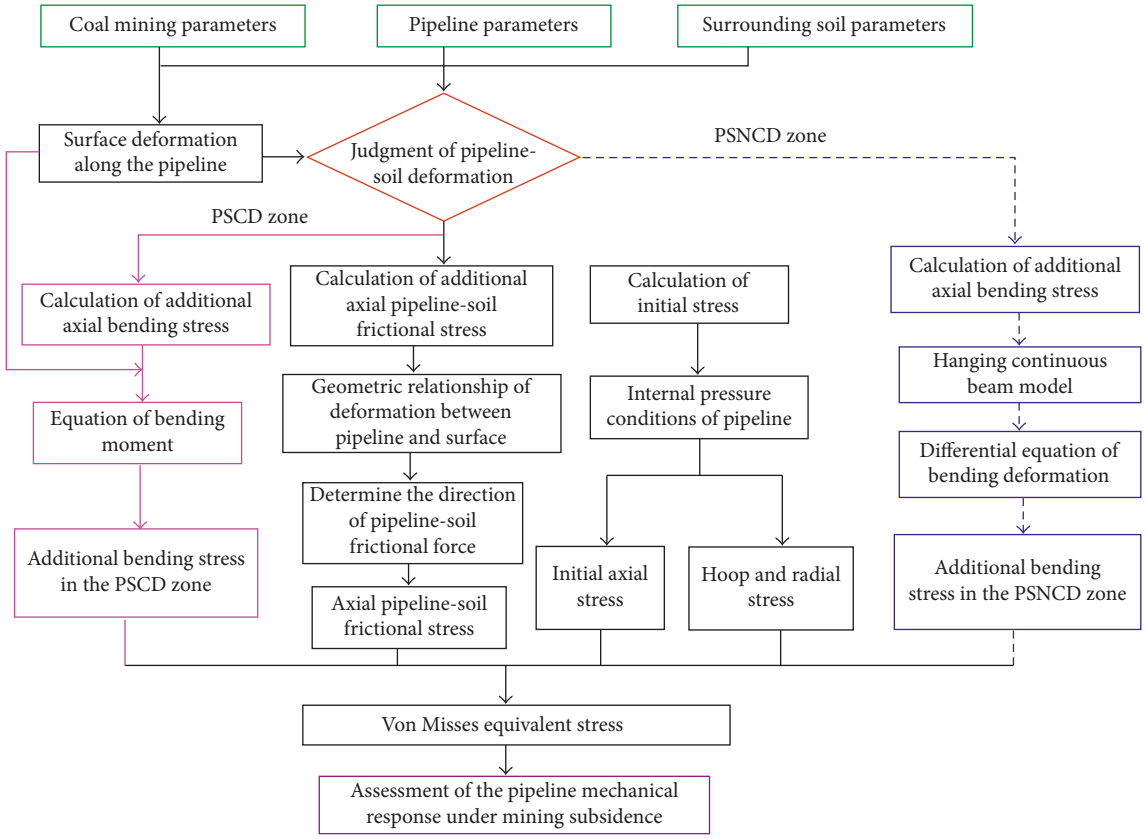


Figure 8: Mechanical response analysis procedure of the buried pipeline.

Table 1: Basic conditions of the 14101 working face.

| Average thickness of coal seam (m) | Dip angle of coal seam (°) | Strike length (m) | Dip length (m) | Depth of coal seam (m) |
|---|---|---|---|---|
| 6.32 | 1–4 | 2640 | 249.5 | 585–603 |

working face was distant from the pipeline. The locations of 14101 working face and buried pipeline through plane projection are shown in Figure 9. The buried natural gas pipeline was made of X60 spiral submerged arc welding steel pipe with 7.1 mm thickness and 660 mm diameter. Meanwhile, the designed working pressure was 6.4 MPa.

*4.2. Surface Deformation along the Buried Pipeline.* According to the mining subsidence prediction parameters of the working face 14101 provided by mine owners in advance listed in Table 2, the mining subsidence could be predicted by the probability integral method which is extensively recommended by correlative regulations of mining subsidence prediction. Consequently, according to the probability integral method and (4)–(7), the surface deformations predicted along the buried pipeline were obtained in advance during the 14101 working face advancing. Surface deformations along the buried pipeline in the mining subsidence zone can be divided into vertical subsidence and horizontal displacement. The evolution of vertical subsidence and horizontal surface displacement perpendicular to the pipeline is shown in Figures 10 and 11, respectively, during the working face

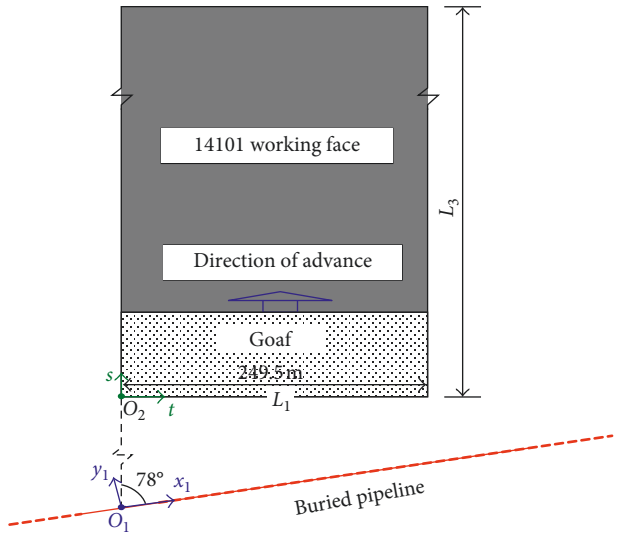


Figure 9: Locations of 14101 working face and buried pipeline through plane projection.

Table 2: Prediction parameters of mining subsidence provided by mine owners.

| Subsidence coefficient, $q$ | Horizontal shift coefficient, $b$ | Tangent of the main influencing angle, tan $\beta$ | Offset distance of the inflection point, $s$ | Mining influence diffusion, $\delta$ |
|---|---|---|---|---|
| 0.85 | 0.28 | 1.8 | 0.18 $H_0$ | 89° |

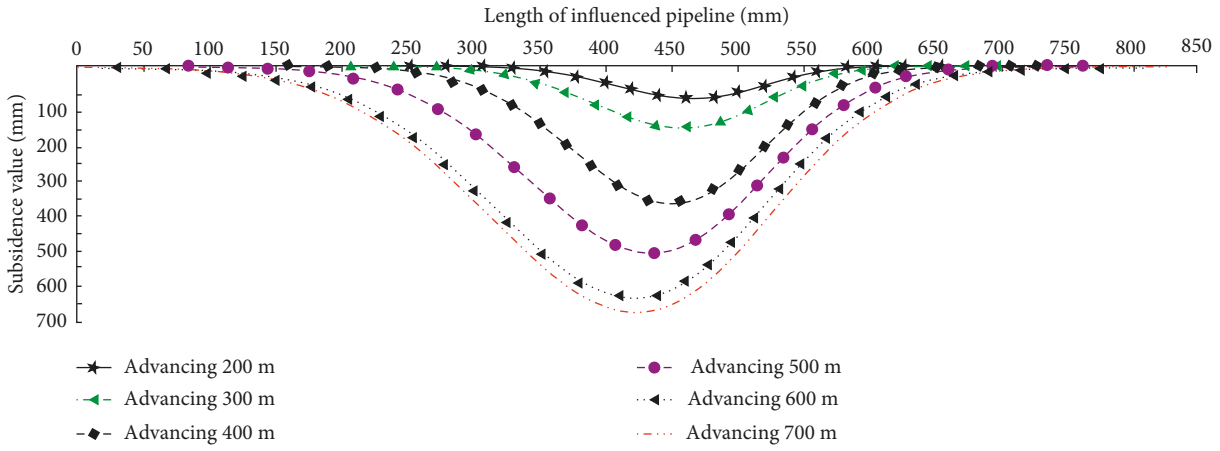


Figure 10: Surface subsidence along the pipeline.

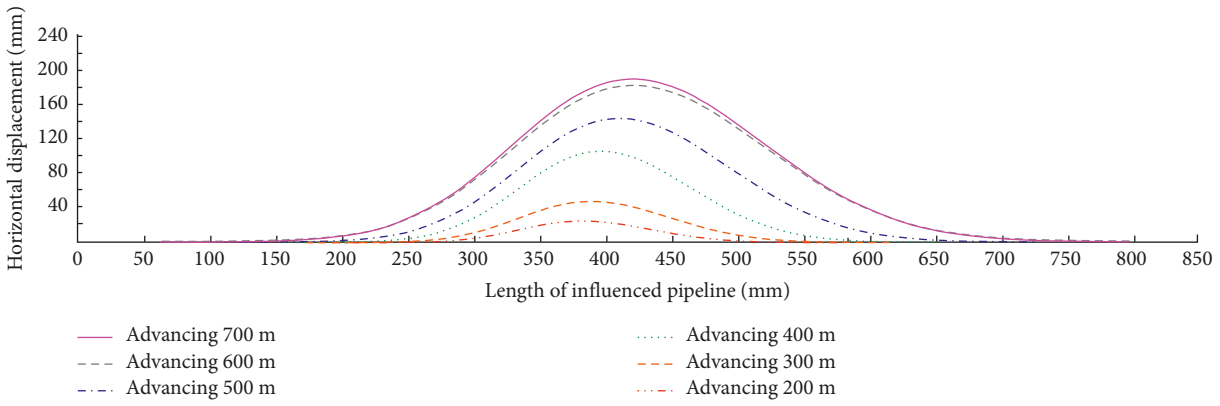


Figure 11: Horizontal surface displacement perpendicular to the pipeline.

advancing. According to the results of the deformation prediction during mining subsidence, the values and ranges of the subsidence along the pipeline would be to maximum and stabilize after the working face advancing for 700 m from the open-off cut, which is as shown in Figures 10 and 11. The $x$-axis direction indicates the increment of the length of the pipeline influenced by subsidence, and the $y$-axis direction indicates the subsidence values and horizontal displacements along the influenced pipeline, respectively, as the coal mine working face exploitation. The maximum length of the buried pipeline influenced by mining is 830 m, the maximum subsidence along the pipeline is approximately 660 mm, and the maximum horizontal displacement is 195 mm after the working face advancing for 700 m.

*4.3. Analysis Result of Additional Stresses on the Pipeline.* The space geometrical locations of the buried natural gas pipeline influenced by mining subsidence and the 14101 working face are shown in Figure 12. According to the

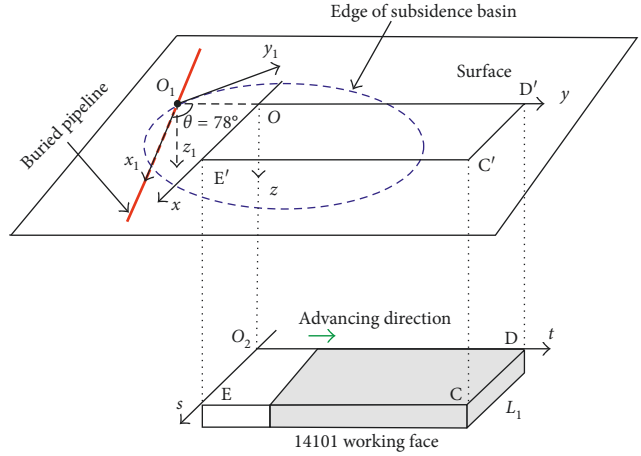


Figure 12: Layout of the 14101 working face and buried pipeline.

Table 3: Physical mechanical parameters of the buried natural gas pipeline.

| Elastic modulus, $E$ (GPa) | Density, $\rho_g$ (kg/m$^3$) | Linear expansion coefficient, $\xi$ | Yield stress, $\sigma_s$ (MPa) | Outer diameter, $D$ (mm) | Thickness, $S$ (mm) | Internal pressure, $P$ (MPa) | Ramberg–Osgood model parameters | |
|---|---|---|---|---|---|---|---|---|
| | | | | | | | $a$ | $n$ |
| 210 | 7,680 | $1.2\times10^{-5}$ | 465 | 660 | 7 | 6.4 | 11 | 24 |

Table 4: Physical and mechanical parameters of the soil around pipeline.

| Density, $\rho_s$ (kg/m$^3$) | Coefficient of soil-pipeline interface, $f'$ | Adhesion coefficient, $k'$ | Coefficient of static earth pressure, $K_0$ | Internal frictional angle, $\psi$ (°) | Cohesion coefficient, $c_s$ (kPa) |
|---|---|---|---|---|---|
| 1,850 | 0.7 | 0.12 | 0.4 | 24 | 23 |

demonstration in 3.2 of this paper, coordinate systems including coal seam, surface, and buried pipeline should be established firstly. The coal seam coordinate system is established in detail as follows: the top left corner of the open-off cut on the 14101 working face is the origin ($O_2$), the dip direction of the coal seam is the $t$-axis, and the strike direction is the $s$-axis. The surface coordinate system ($Oxy$) is a projection of the coal seam coordinate system ($O_2st$) on the surface. The created pipeline coordinate system uses the intersection point between the buried pipeline and $y$-axis of the surface coordinate system as the origin ($O_1$), and the pipeline extension is the $x_1$-axis. According to the locations of working face 14101 and pipeline, the $O_1$ coordinates in the surface coordinate system are (0, −176), and the included angle between the $x_1$- and $y$-axes is 78°.

As illustrated in mechanical response analysis procedure (Figure 8), the PSCD should be analyzed after the surface deformation along the buried pipeline obtained. Subsequently, critical conditions of PSCD can be derived by (2) and additional stresses on the buried pipeline could be obtained by previously proposed analysis process in Figure 8 during the 14101 working face advancing. Given many parameters and the adaptively programmed calculation process for the stress analysis, a MATHEMATIC programming for the additional stress calculations of the buried pipeline influenced by the 14101 working face advancing can be obtained according to the analysis process proposed in Figure 8. The parameters mainly comprise three aspects as shown in Figure 8 which are, respectively, coal mining parameters listed in Tables 1 and 2, pipeline parameters listed in Table 3, and surrounding soil parameters listed in Table 4. It is worth to declare that the parameters in Table 2 are just for deformation prediction along the pipeline based on the probability integral method. The pipeline parameters include physical mechanical parameters as well as the constitutive relationship parameters of the pipeline material listed in Table 3. The constitutive relationship of the material of buried natural gas pipeline which is steel adopts the Ramberg–Osgood model shown as follows [24]:

$$\varepsilon = \frac{\sigma}{E_0}\left[1 + \frac{n}{1+a}\left(\frac{\sigma}{\sigma_n}\right)^a\right], \tag{28}$$

where $E_0$ is the initial elastic modulus the steel pipeline, $\sigma_n$ is the yield stress of the steel pipeline, and $n$ and $a$ are the Ramberg–Osgood model parameters listed in Table 3.

The results obtained according to the analysis process proposed in Figure 8 indicate that pipeline and surrounding soil mass maintain the coordinating deformation during the 14101 working face advancing. Taking into account the modes of additional bending and pipeline-soil frictional force, it is easy to get that the maximum additional stress of the pipeline will be generated along the top or bottom of the buried pipeline according to superposition theory during mining subsidence process. Therefore, it is more meaningful to analyze the additional stress along the top or bottom of the buried pipeline. According to the analysis process proposed in Figure 8 after the deformations of pipeline, the coal mining parameters, pipeline parameters, and surrounding soil parameters obtained, the additional stresses are obtained along the top or bottom of the buried pipeline during the 14101 working face advancing which are shown in Figures 13(a) and 13(b).

As can be seen in Figure 13, the maximum additional compression stresses are 52.1, 83.2, 132.5, 156.7, 170.2, and 172.8 MPa when the working face advancing is 200, 300, 400, 500, 600, and 700 m, and the maximum additional tensile stresses are 45.3, 69.2, 80.3, 99.6, 114.3, and 115.8 MPa, respectively, under mining subsidence. Given the additional bending stress, the pipeline is tensioned on the top and compressed at the bottom along the pipeline on the edge of the subsidence zone, where the axial stress caused by friction is tensile stress. Therefore, it would be a rapid increment for the tensile stress on the top pipeline via the superposition of additional bending stress and friction. For the same reason, the pipeline is compressed by the bending stress at the top but tensioned at the bottom in the middle of the subsidence zone, while the axial stress caused by pipeline-soil friction is a compression stress in this zone. Thus, the bending compression stress and pipeline-soil frictional force in the middle of the subsidence zone are superimposed at the top of the pipeline. As can be seen in Figure 13, it is easy to know that there are three stress peaks on the two edges and middle of the subsidence zone where the most vulnerable regions to the buried pipeline are located.

*4.4. Comparative Analysis of Additional Stresses between Simulation and Calculation.* The deformation along the buried pipeline is ultimately induced by the strata movement upon the coal seam during the working face excavation.

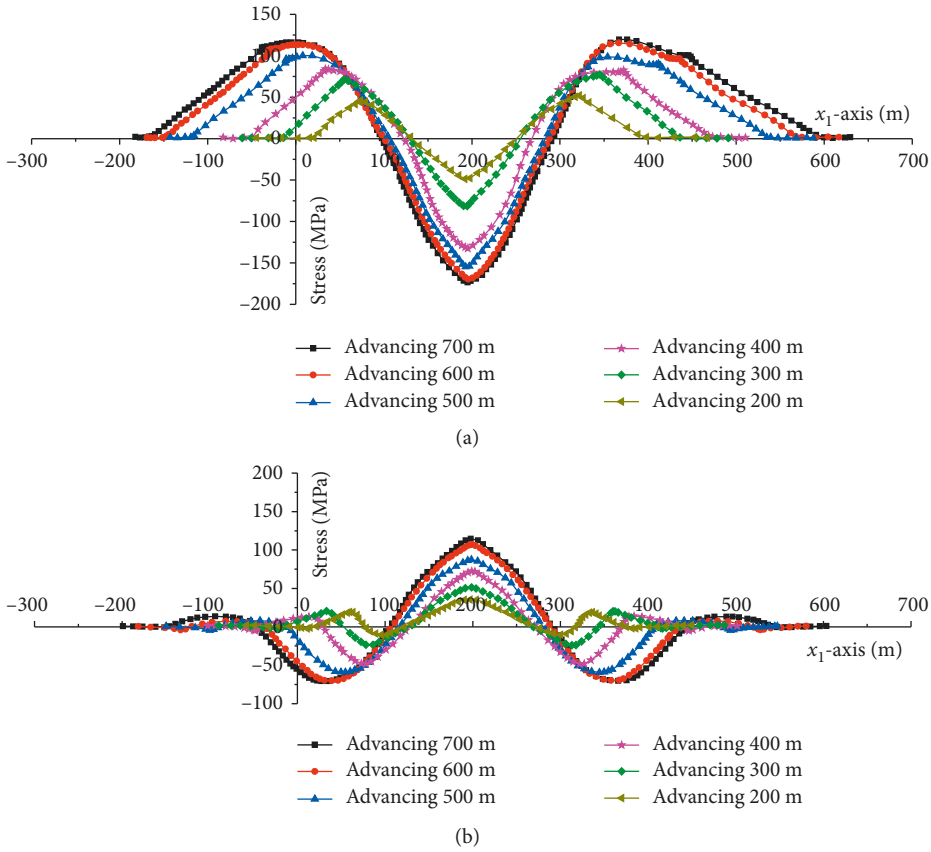


Figure 13: Additional axial stresses on the buried pipeline as the working face advancing: (a) axial stresses distribution on the top of the pipeline and (b) axial stresses distribution at the bottom of the pipeline.

However, if the excavation is used directly in the simulation model, the realistic surface deformation caused by the working face excavation is hard to come by because of the irrealizable simulation to the randomness distributions of the joints, cracks, fault, groundwater, ground stress, and so forth. However, the exiting researches shown that the additional stress on the buried pipeline affected by surface deformation is exactly as a result of the soil-pipeline interaction which may be implemented by the contact modeling [25]. The interaction between the pipeline and its surrounding soil mass is implemented by the contact modeling in this simulation analysis. The master-slave contact provided by ABAQUS (Version 6.9) is used to realize the pipe-soil interaction in subsidence soil. The master and slave surfaces are defined as the contact of pipeline and its surrounding soil, respectively. The pipeline-soil interaction includes a normal force (earth pressure around the pipeline) and a tangential force (frictional resistance at the pipeline-soil interface). It is worth to declare that a "HARD" contact is used which can exert normal and shear stresses (pipeline-soil frictional force), what is more, the utmost frictional force defined by Coulomb model between pipeline and its surrounding soil. The details about establishment process of a specific contact modeling in simulation analysis were illuminated in the published literatures [17, 18].

According the scope of the subsidence area, the size of the simulation model adopted is 1200 (length) × 8 (depth) × 6 (width). The displacement controlled loading to the surface is used in this simulation since the available surface deformations along the pipeline obtained in advance are shown in Figures 10 and 11. In order to implement the actual surface deformations along the pipeline, the model is divided into subsidence and nonsubsidence areas based on the scope of the subsidence (Figure 14). Subsequently, the two horizontal constraints are removed while the horizontal surface displacement as shown in Figure 10 is added to the model by displacement controlled loading. Similarly, the surface subsidence along the pipeline is added to the model. The graphical modeling approach and displacement controlled loading to the buried pipeline and soil mass is briefly illuminated in Figure 14.

When the different deformations and scopes of subsidence zones added to the simulation model, the corresponding outputs about the additional stresses on pipeline and pipeline-soil deformations along the affected pipeline during subsidence will be obtained. Given the same implementation procedure in PSCD stage, we just take the results of the deformation and stresses after the working face advancing for 700 m (length of the buried pipeline influenced by mining is 830 m) to clarify the influence of subsidence which is shown in Figure 15. The distribution and development of the deformations about buried pipeline and its surrounding soil are synchronously shown in displacement nephogram (Figure 15(a)). As can be seen in Figure 15(a), the

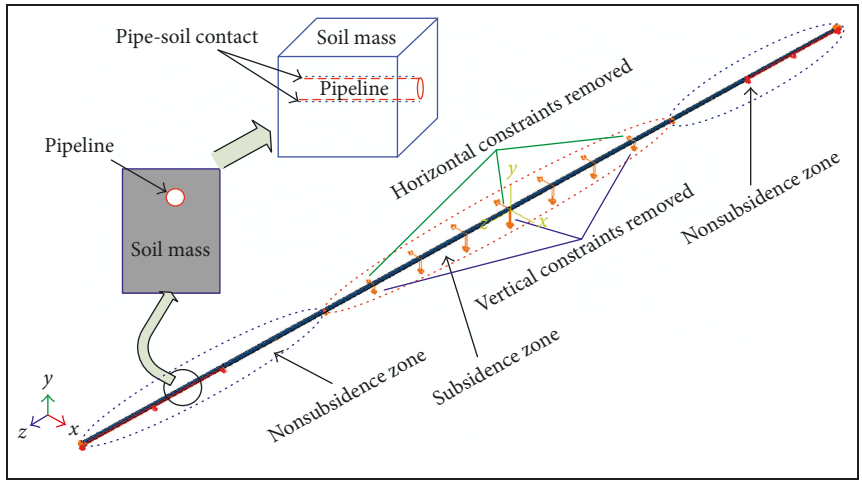


Figure 14: Simulation model and displacement loading.

PSCD based on the predication results is obtained through the simulation. Subsequently, the additional stress distribution along the buried pipeline is presented and the additional stresses on pipeline in special locations are also sketched in Figure 15(b). As can be seen in Figure 15(b), the maximum additional stress of the pipeline is generated along the top or bottom of the buried pipeline, what is more, three stress peaks on the two edges and middle of the subsidence basin. Obviously, the characteristic of additional stress and deformation presented by simulation is identical with previous results through analytical calculation.

In order to present comparison results between the analytical calculation and the simulation, the additional stresses extracted from the top and the bottom of the pipeline during subsidence induced by the working face advancing are shown in Figure 16. In comparison with Figure 13, the distribution rule of the additional stresses is similar to the results of analytical calculation, which also have three stress peaks on the two edges and middle of the subsidence basin. However, there are some differences between the simulation results (Figure 16) and calculation results (Figure 13), and the curves of addition stresses along the pipeline by simulation are more smooth compared with those of Figure 13 deduced by analytical calculation. It is because of the handling to the calculation of the pipeline-soil frictional force. More specifically, the assumption and simplification to the distribution and calculation of frictional force result in the different stress curves along the buried pipeline in the subsidence zone. As previously mentioned, the distribution of frictional force along the pipeline is simplified as shown in Figure 7 in the analytical calculation. In addition, the frictional force is deduced by the ultimate formulas as shown in (19) as pipeline-soil relative displacement is big enough to reach yield displacement along the buried pipeline influenced by mining subsidence. In contrast, there will be a uniform and slow variation to the pipeline-soil frictional force because of the contact and Coulomb model defined between pipeline and its surrounding soil in simulation analysis. It is necessary to declare that the uniform and slow variation to the pipeline-soil frictional force in simulation is not an actual situation because of the fact that the relative displacements happened actually between pipeline and its surrounding soil will be generally much bigger than yield pipeline-soil displacement (about 3–10 mm) during mining subsidence.

Obviously, on the basis of the analysis above, there will have some differences about the additional stress values especially at the two edges of the subsidence zone between Figures 14 and 16. According to the process of getting pipeline-soil frictional force, a maximum frictional force (ultimate frictional force) on pipeline is always generated by the analytical calculation other than a uniform decreasing frictional force generated by simulation at the two edges of the subsidence area. Therefore, there will be some visible differences to the additional stress shown in Figures 13 and 16 after the superposition of additional frictional stress and bending stress at those areas. However, the differences of additional stress obtained by the two methods are still not very large because both frictional stress and bending stress are small at those areas. In the middle of the subsidence area where the maximal additional stress is generated, the differences of additional stress obtained by the two methods are also confined to small values because of the fact that the frictional force close to the ultimate frictional force will be generated in simulation. In comparison with the results deduced by analytical calculation which is shown in Figure 13, the maximum discrepancies of maximum additional compression and tensile stresses obtained by simulation to the stresses deduced by analytical calculation are only 9.38% and 16.23%, respectively.

Taking into account the above comparative analysis between simulation and analytical calculation, the following conclusions can be made: (1) the distribution of additional stresses obtained by simulation and calculation along the pipeline are similar, and there are three stress peaks on the two edges and middle of the subsidence zone; (2) there will have some differences about the additional stress values especially at the two edges of the subsidence area between the two methods because of the different handling to the pipeline-soil frictional force; (3) the maximum additional stresses proposed by simulation analysis are close to the

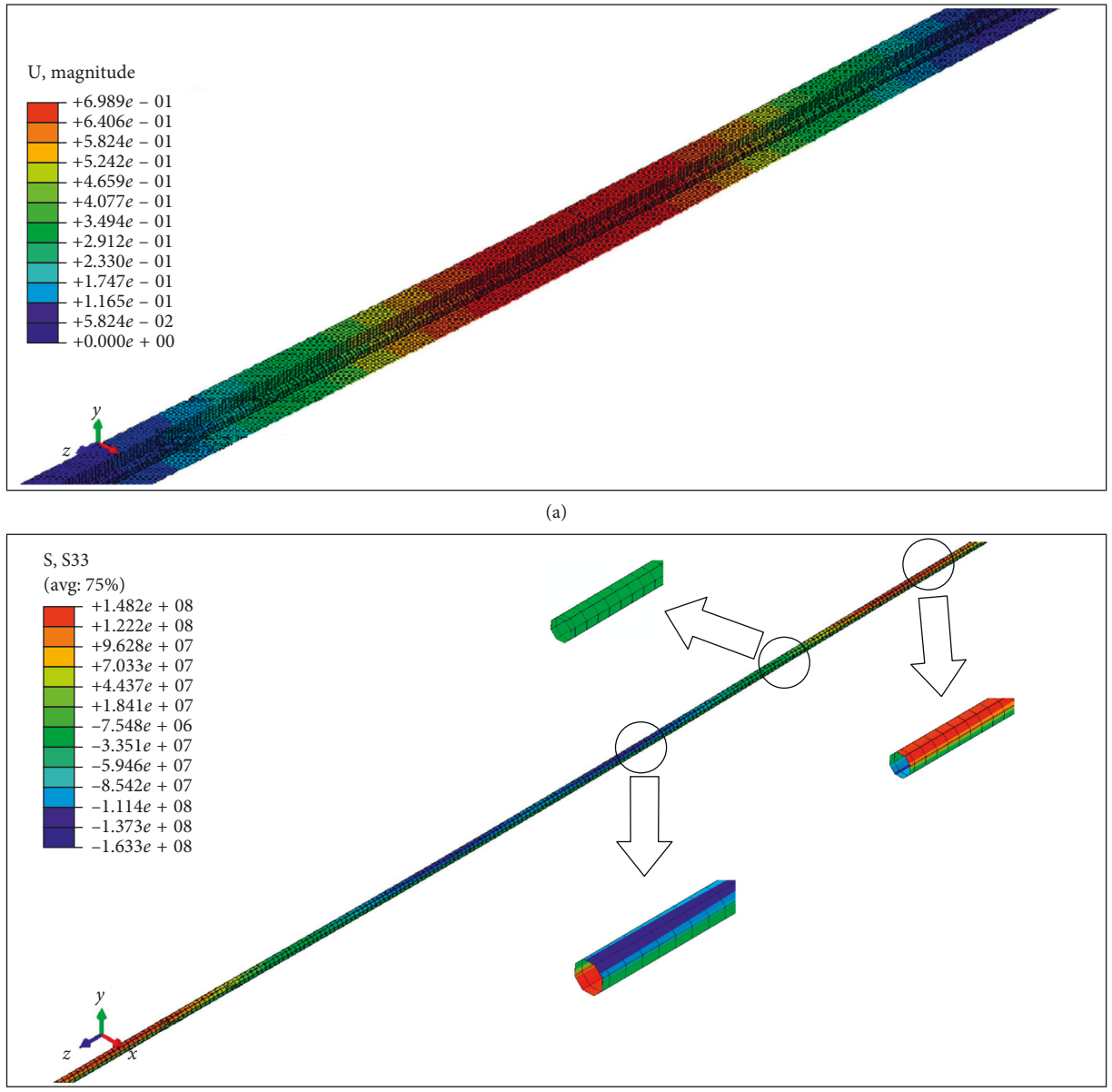


Figure 15: Deformations and additional stresses along the buried pipeline: (a) distribution of the deformations about buried pipeline and its surrounding soil and (b) additional stress distribution along the buried pipeline.

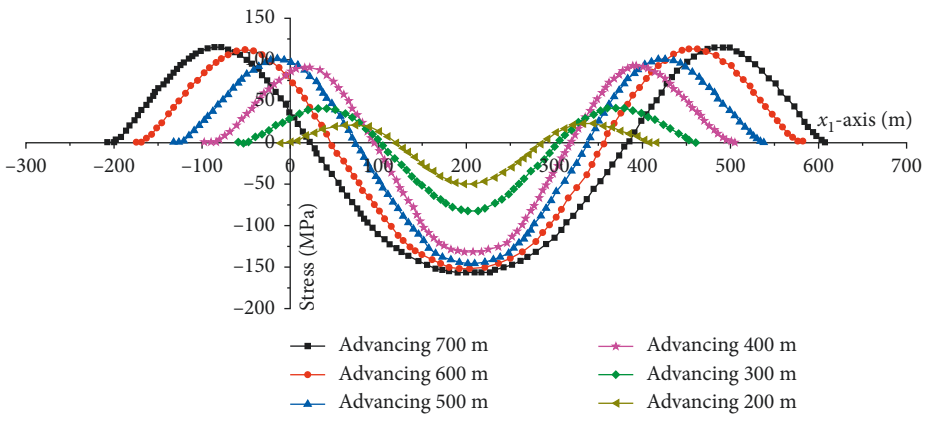


(a)

Figure 16: Continued.

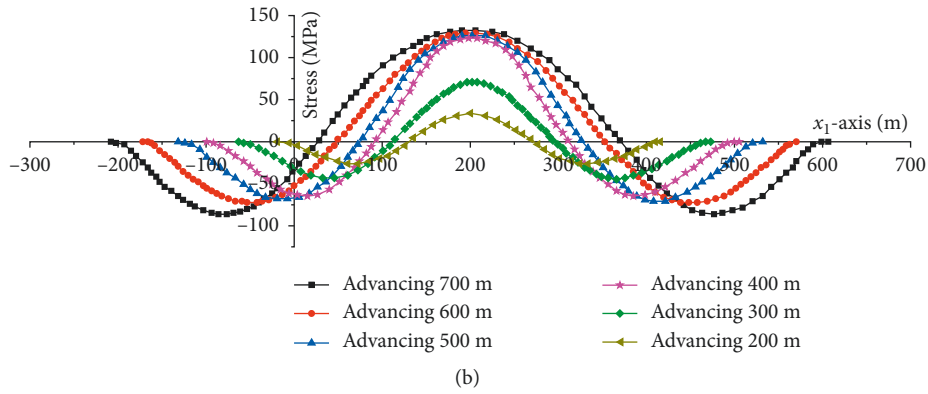


Figure 16: Additional axial stresses along the pipeline presented by simulation: (a) axial stresses distribution on the top of the pipeline and (b) axial stresses distribution at the bottom of the pipeline.

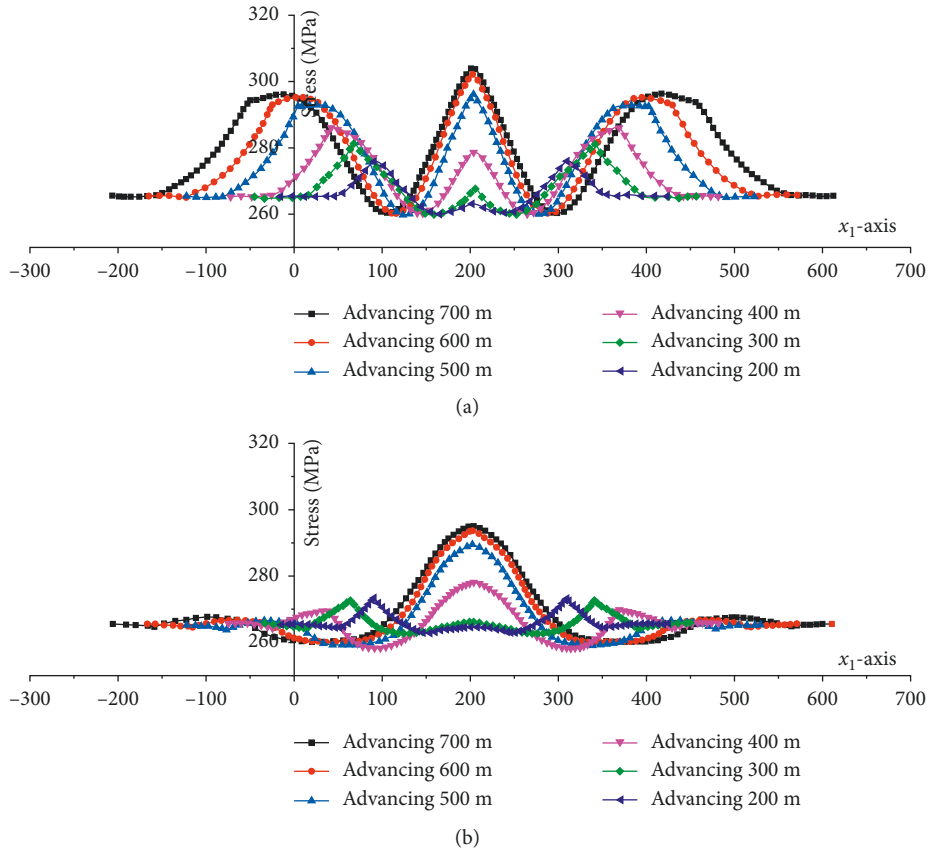


Figure 17: Von Mises stresses of the buried pipeline as the working face advancing: (a) Von Mises stresses distribution on the top of the pipeline and (b) Von Mises stresses distribution at the bottom of the pipeline.

analytical calculation results presented in Figure 13. So, it is concluded that the additional stresses on the buried pipeline deduced by analytical calculation based on PSCD are available and reliable. It is worth to mention that the derivations of additional stresses are according to the surface deformations along the pipeline which could be predicted in advance according to the prediction parameters of mining subsidence. Therefore, the methodology proposed in this paper is more conveniently and easily applied in practical work to evaluate the influence of surface subsidence to buried pipelines because the surface deformation will be generally available in advance during the evaluation of the mining damage.

*4.5. Von Mises Equivalent Stresses on the Buried Pipeline.* The strength design of the buried pipelines follows the stress-based criterion. In particular, the maximum stresses along

the pipelines are smaller than the yield stress to ensure the pipeline operation and construction requirements. Considering the yield characteristics of pipeline steel and effect of the additional axial stress in the mining subsidence process, the Von Mises equivalent stress is often used to evaluate the yield state of pipeline steel.

The Von Mises equivalent stresses on the top and at the bottom of the buried pipeline can be obtained by combining the additional stresses of the pipeline in Figure 13 and the initial stress of the pipeline deduced by (22)–(24) when the 14101 working face advancing (Figure 17). As can be seen in Figure 17, there are also three peaks of Von Mises stress just as the additional stress on the edges and middle of the subsidence zone along the buried pipeline as the 14101 working face advancing. The additional stresses of the buried pipeline are composed of bending and axial pipeline-soil frictional stresses under the influence of mining subsidence. What is more, the axial frictional stress is a pipeline-soil ultimate frictional force simplified during analytical calculation in this paper. At the change points of the frictional force direction, axial additional stresses and Von Mises equivalent stresses will change more suddenly as shown in Figures 13 and 17.

According to the initial stress deduced by (22)–(24), the initial Von Mises stress on the buried pipeline is 264 MPa before mining subsidence. However, with the influence of mining subsidence, the maximum Von Mises stress on the top of the pipeline is 305.2 MPa as well as the maximum Von Mises stress at the bottom of the pipeline is 294.8 MPa. Combined with the yield strength of pipeline steel listed in Table 3, the maximum Von Mises stress along the buried pipeline under the influence of mining subsidence is $\sigma_{\text{Mises-max}} = 305.2\ \text{MPa} < [\sigma_s] = 465\ \text{MPa}$. The calculation results indicated that the maximum Von Mises equivalent stress is smaller than the yield stress as the 14010 working face advancing. However, it is necessary to declare that the additional stress deduced by simulation or analytical calculation during subsidence mainly considered influence of the pipeline and its surrounding soil deformations, so this comparison result between $\sigma_{\text{Mises-max}}$ and $[\sigma_s]$ is not as an ultimate safety estimation to buried pipeline although the $\sigma_{\text{Mises-max}} < [\sigma_s]$, because there are some variations of influences unconsidered to the buried pipeline. Nevertheless, the results presented by analytical calculation in this paper are obviously a significant evidence to the buried pipeline safety and hazard estimation, because the analysis process of additional stresses is according to the pipeline-soil deformation which is an essential influence to additional stresses of the buried pipeline during mining subsidence.

## 5. Conclusions

The objective of this study is to aid to the development of the additional stress analysis method and process for safety estimation of buried pipeline affected by mining subsidence. A stress analysis method and process of the buried pipeline are presented during mining subsidence. The key points and conclusions of the study are as follows:

(1) The relationship of pipe-soil coordinating deformation should be defined in advance during mining subsidence, and the evolution of additional stresses of the buried pipelines and deformations can be reflected comprehensively by the segmented mechanical models established in this paper according to the PSCD and PSNCD.

(2) The geometric relationships between surface deformations caused by mining subsidence and buried pipeline deformation are established. Subsequently, an available programming analysis process to the mechanical response analysis procedure of the buried pipeline has been also been presented in Figure 8 which takes the additional axial bending stress, pipeline-soil frictional force, initial stress, and Von Mises stress into account.

(3) Additional stresses of a buried pipeline under the influence of mining subsidence as the 14101 working face advancing are calculated via programming according to the mechanical response analysis procedure (Figure 8). The results show that the maximum Von Mises stress is smaller than the yield stress of the pipelines; however, three peaks of additional and Von Mises stresses of the buried pipeline deduced by simulation and analytical calculation locate in the edges and middle of the subsidence curve, and these positions are the most vulnerable places to the buried pipeline.

The method proposed in this paper would be certainly more suitable for overall safety and hazard estimation to buried pipelines affected by mining subsidence if combined with other influences such as the variations of soil properties and construction conditions of the pipeline in future researches.

## Conflicts of Interest

The authors declare that there are no conflicts of interest regarding the publication of this paper.

## Acknowledgments

Financial support from the National Natural Science Foundation of China (nos. 51504081 and 51508166), the Scientific and Technological Research Projects of Henan Province China (no. 162102210221), and the Doctor Foundation of Henan Polytechnic University (no. B2016-67) is gratefully appreciated. Ping Xu would like to thank the University of Western Australia for a Visiting Professorship at UWA from 2016 to 2017.

## References

[1] A. Saeidi, O. Deck, and T. Verdel, "Comparison of building damage assessment methods for risk analysis in mining subsidence regions," *Geotechnical and Geological Engineering*, vol. 31, no. 4, pp. 1073–1088, 2013.

[2] X. Zhu, G. Guo, J. Zha, T. Chen, Q. Fang, and X. Yang, "Surface dynamic subsidence prediction model of solid

backfill mining," *Environmental Earth Sciences*, vol. 75, p. 1007, 2016.

[3] X. Diao, K. Wu, D. Hu, L. Li, and D. Zhou, "Combining differential SAR interferometry and the probability integral method for three-dimensional deformation monitoring of mining areas," *International Journal of Remote Sensing*, vol. 37, no. 21, pp. 5196–5212, 2016.

[4] H. D. Fan, W. Gu, Y. Qin, J. Q. Xue, and B. Q Chen, "A model for extracting large deformation mining subsidence using D-InSAR technique and probability integral method," *Transactions of Nonferrous Metals Society of China*, vol. 24, no. 4, pp. 1242–1247, 2014.

[5] Y. Liu, F. Zhou, X. Geng et al., "A prediction model and numerical simulation of the location of the longwall face during the highest possible failure period of gob gas vent-holes," *Journal of Natural Gas Science and Engineering*, vol. 37, pp. 178–191, 2017.

[6] S. Joshi, A. Prashant, A. Deb, and S. K. Jain, "Analysis of buried pipelines subjected to reverse fault motion," *Soil Dynamics and Earthquake Engineering*, vol. 31, no. 7, pp. 930–940, 2011.

[7] J. Y. Zheng, B. J. Zhang, P. F. Liu, and L. L. Wu, "Failure analysis and safety evaluation of buried pipeline due to deflection of landslide process," *Engineering Failure Analysis*, vol. 25, pp. 156–168, 2012.

[8] J. Yu, C. Zhang, and M. Huang, "Soil-pipe interaction due to tunnelling: assessment of Winkler modulus for underground pipelines," *Computers and Geotechnics*, vol. 50, pp. 17–28, 2013.

[9] L. Zhang, X. Wu, Q. Chen, M. Skibniewski, and J. Zhong, "Developing a cloud model based risk assessment methodology for tunnel-induced damage to existing pipelines," *Stochastic Environmental Research and Risk Assessment*, vol. 29, no. 2, pp. 513–526, 2015.

[10] Z. Zhang and M. Zhang, "Mechanical effects of tunneling on adjacent pipelines based on Galerkin solution and layered transfer matrix solution," *Soils and Foundations*, vol. 53, no. 4, pp. 557–568, 2013.

[11] L. J. Prendergast and K. Gavin, "A comparison of initial stiffness formulations for small-strain soil-pile dynamic Winkler modeling," *Soil Dynamic and Earthquake Engineering*, vol. 81, pp. 27–41, 2016.

[12] S. S. Peng and Y. Luo, "Determination of stress field in buried thin pipelines resulting from ground subsidence due to longwall mining," *Mining Science and Technology*, vol. 6, no. 2, pp. 205–216, 1988.

[13] A. A. Malinowska, "Fuzzy inference-based approach to the mining-induced pipeline failure estimation," *Natural Hazards*, vol. 85, no. 1, pp. 621–636, 2017.

[14] A. A. Malinowska, "Reliability of methods used for pipeline hazard evaluation in view of potential risk factors," *Natural Hazards*, vol. 83, no. 1, pp. 715–728, 2016.

[15] X. L. Wang, J. Shuai, and J. Q. Zhang, "Mechanical response analysis of buried pipeline crossing mining subsidence area," *Rock and Soil Mechanics*, vol. 32, no. 11, pp. 3373–3378, 2011, in Chinese.

[16] Y. F. Zou, *Mining Subsidence Engineering*, China University of Mining and Technology Press, Xuzhou, China, 2003, in Chinese.

[17] P. Xu, *Study on the Buried Pipeline-Soil Interaction and Its Mechanical Response by Mining Subsidence*, Ph.D. dissertation, University of Mining and Technology, Xuzhou, China, 2015, in Chinese.

[18] P. Xu, M. X. Zhang, W. J. Cui, and S. Gao, "Experimental study of buried pipeline-soil interaction induced by subsidence," *Industrial Construction*, vol. 12, pp. 67–72, 2016, in Chinese.

[19] X. L. Wang and A. L. Yao, "Deflection and internal force analysis of buried steel pipeline in partial hanging," *Engineering Mechanics*, vol. 8, pp. 218–222, 2008, in Chinese.

[20] V. E. Melissianos and C. J. Gantes, "Buckling and post-buckling behavior of beams with internal flexible joints resting on elastic foundation modeling buried pipelines," *Structures*, vol. 7, pp. 138–152, 2016.

[21] J. D. Nyman, *Guidelines for the Seismic Design of Oil and Gas Pipeline Systems*, Committee on Gas and Liquid Fuel Lifelines, ASCE, Reston, VA, USA, 1984.

[22] T. D. O'Rourke, J. K. Jung, and C. Argyrou, "Underground pipeline response to earthquake-induced ground deformation," *Soil Dynamics and Earthquake Engineering*, vol. 91, pp. 272–283, 2016.

[23] Y. J. Tang, *Stress Analysis of Pressure Pipeline*, Sinopec press, Beijing, China, 2003, in Chinese.

[24] D. K. Karamitros, G. D. Bouckovalas, and G. P. Kouretzis, "Stress analysis of buried steel pipelines at strike-slip fault crossings," *Soil Dynamics and Earthquake Engineering*, vol. 27, no. 3, pp. 200–211, 2007.

[25] L. Zhang, X. B. Zhao, X. Z. Yan, and X. J. Yang, "A new finite element model of buried steel pipelines crossing strike-slip faults considering equivalent boundary springs," *Engineering Structures*, vol. 123, pp. 30–44, 2016.